



Thrust fault reflections on wide-angle seismics: Modeling by a new approach and implications to Neoproterozoic collision

Gopala Krishna Velamakanni^{1,2} and Vijaya Rao Vaidya^{1,3}

¹CSIR - National Geophysical Research Institute, Hyderabad-500007, India;

²gopalakrishna.velamakanni@gmail.com **ORCID iD** <https://orcid.org/0000-0003-2178-4847>

³vijayraov@yahoo.co.in **ORCID iD** <https://orcid.org/0000-0002-9314-231X>

Abstract

Collisional events contemporaneous to the global Grenvillian (~1.1 Ga) and the East African (~550 Ma) orogens created a major fold and thrust belt system in the south Indian shield. The Cuddapah basin Eastern Boundary Thrust (CEBT), a significant part of this system, is believed to have evolved by fragmentation and amalgamation of continental blocks in this region. The Cuddapah basin in the eastern Dharwar craton of south India has a long Paleo-Neoproterozoic geological history. Deep seismic near-vertical reflection profiling is the most successful geophysical technique utilized to delineate such complex crustal structures of the orogens. Here we utilize observations on a refraction /wide-angle reflection profile for the first time, to delineate the structure of the CEBT. We developed a novel modeling approach for this purpose utilizing the '**localized phantom horizons**' consistent with the limited-extent discrete reflector segments of the continental crust in the region. A detailed velocity model and geometry of the structure inferred here, by synthetic seismograms modeling of unequivocal seismic reflections, provide clues on the evolution of the CEBT. Another thrust, the Eastern Ghats Thrust (EGT), related to the Eastern Ghats orogen, contemporaneous with the Columbia supercontinent is also identified. Integrating these modeling results, inferred velocity structure, observed steep gradient bipolar gravity anomaly and other geological data, we interpret the CEBT as a collisional suture juxtaposing the Cuddapah basin and the Eastern Ghats mobile belt.

Keywords: Continental crust, Cuddapah basin - south India, Seismic Wide-angle Reflections, Localized phantom horizons modeling approach, Collisional Suture



26 **Short Summary:**

27 A novel modeling approach of crustal seismics is developed for deep crustal structure and velocity model
28 using **localized phantom horizons**. We model two boundary thrusts at margins of Cuddapah basin and
29 Eastern Ghats Belt formed over the Indian shield during the Rodinia and Columbia supercontinental
30 episodes (1.1Ga and 1.8Ga). The results are significant to continental evolution. Imprints of collisional
31 orogeny revealed as two thrust faults on the margins of the structures involved are modelled.

32 **1. Introduction**

33 Subduction, collision and suturing of crustal blocks, responsible for evolution of the orogens, are
34 the underlying processes for formation of the supercontinents. Collisional tectonics provides the
35 fundamental stress mechanism for the generation of large thrusts at the boundaries of colliding crustal
36 blocks during crustal evolution. Low-angle thrust-faults are the reverse faults having finite length and
37 breadth, dipping at a low-angle of $< 45^\circ$ or even smaller. Variable dipping reverse faults do occur in
38 nature because of variations in the rock properties on a fault surface. Figures 1a and b, illustrate the typical
39 images of prominent thrust faults delineated on seismic reflection profiles in the Indian and the Canadian
40 shields (Cook, 2002; Mandal et al., 2014).

41 Most of the Precambrian crust of the Indian shield was formed and reworked over several orogenic
42 events since Neoproterozoic. Many of these events were associated with the assembly and breakup of super-
43 continents. One such area is the southern part of the Indian shield, where the Proterozoic Cuddapah basin
44 spreading across $\sim 45,000 \text{ km}^2$ is located (Figure 2). It was subjected to compressional forces leading to
45 the formation of an orogen and a thrust fault at its eastern margin. Here, we use the seismic refraction /
46 wide-angle reflection data acquired along the Deep Seismic Sounding (DSS) profile across the Cuddapah
47 basin by continuous profiling technique with closely spaced 100 m geophone interval. The acquisition
48 geometry by this technique ensured dense overlapping and reverse data coverage on this profile,
49 especially the reflections from the thrust fault. In the present study we model these high-amplitude and
50 high-apparent velocity reflections, significantly observed similar to the Moho reflection phase on this
51 profile, to determine the velocity structure and geometry of the thrust-fault for the first time even in the



52 absence of a conventional near-vertical reflection seismic profile. We present detailed modeling of
53 seismic wide-angle reflections, interpreting them due to a collisional low-angle thrust fault on the eastern
54 margin of the Proterozoic Cuddapah basin, referred here as the Cuddapah basin Eastern Boundary Thrust,
55 (CEBT). Delineation of the “Thrust Fault” on the eastern margin of the Cuddapah basin as significantly
56 revealed on a refraction / wide-angle reflection seismic dataset across it, is the main objective of the
57 present study. The results have significance on a global perspective of the continental crustal evolution
58 and correlation as also revealing the potential of dense wide-angle seismic observations and their
59 modelling by novel techniques.

60 Significant wide-angle reflections from the thrust faults, prominently observed on a few specific
61 favourably oriented refraction profiles, are illustrated in Figures 1c and d. We develop here a new
62 modeling approach to utilize these wide-angle reflections and generate their matching synthetics in order
63 to unravel the geometry and structure of the CEBT with its plausible geodynamic implications. This new
64 approach is also suitable to consider adequately the presence of limited-extent discrete reflectors in the
65 crust inferred earlier in this region from the refraction data. The seismic structure delineated here is further
66 used to infer a viable model of the crustal evolution consistent with other observations in the region. We
67 are of the opinion that this method in a long way may reconcile the differences between the seismic
68 structures derived from near-vertical and refraction data sets.

69 **2. Geology and Tectonics**

70 The Mesoarchean Dharwar craton in south India is one of the largest and oldest cratonic blocks in
71 the world like the Superior, the Yilgarn and the Kaapval cratons. It is divided into two distinct blocks
72 namely, the Mesoarchean Western Dharwar Craton and the Neoarchean Eastern Dharwar Craton (EDC).
73 Among these two crustal blocks, the Western Dharwar Craton was relatively stable, whereas the Eastern
74 Dharwar Craton exhibits episodic growth since Neoarchean; including formation of the Cuddapah basin
75 (1.8 - 0.550 Ga), evolution of fold belts, formation of granulite facies metamorphism, magmatism
76 manifested in the form of mafic dykes (1.8 - 1.1 Ga) and Kimberlite pipes (Kumar et al., 1993; Kale et



77 al., 2020; Saha and Tripathy, 2012). Tectonic framework of the Eastern Dharwar craton is shown in Table
78 1.

79 The crescent shaped Cuddapah basin located along the eastern margin of the EDC is one of the
80 largest Indian cratonic basins (Figure 2). The N-S trending Cuddapah basin extends for a length of about
81 450 km along the arcuate eastern margin with ~150 km mean width. It has a long Paleo-Neoproterozoic
82 geological history and hosts a large number of mineral deposits. Based on the sedimentation pattern,
83 spatial distribution and age six sub-basins are suggested within the Cuddapah basin (Ramam and Murthy,
84 1987), namely, the Palnad, Srisailem, Kurnool, Nallamalai, Chitravati and Papagni- sub-basins (Figure
85 2). The Nallamalai subgroup located in the eastern part of the basin hosts a thick shallow marine
86 succession that is intensely deformed. It represents a N-S trending fold-and-thrust belt referred as the
87 Nallamalai Fold Belt (NFB). The other subbasins located to its west host relatively undeformed and
88 unmetamorphosed sediments. The Nellore Schist Belt (NSB) and Eastern Ghats Belt (EGB) are the two
89 major tectonic domains located to the east of NFB of the Cuddapah basin.

90 The Neoarchean Nellore Schist Belt (Ravikant, 2010) is ~300 km long composite tectono-
91 stratigraphic unit comprising greenschist to amphibolite facies volcano-sedimentary rocks intruded by
92 granites and alkaline plutons (Prakasham Alkaline Province). Two small ophiolitic slivers, namely 1.9
93 Ga Kandra Ophiolite Complex and 1.33 Ga Kanigiri Ophiolitic Melange are also intruded into the NSB
94 during Paleo- and Mesoproterozoic period respectively (Vijaya Kumar et al., 2010; DharmaRao et al.,
95 2011). Multiple cycles of deformation and metamorphism have affected the Nellore Schist Belt (NSB).
96 The Eastern Ghats Belt is a poly-metamorphosed, multi-deformed deeply eroded part of an extensive
97 orogenic belt located along the eastern margins of the Archean cratons of India. The 1000 km long N-S
98 trending Late Proterozoic orogen consists of supracrustals and igneous rocks. It is composed of mafic and
99 felsic granulites (charnokites), anorthosites and alkaline rocks. The Eastern Ghats Belt is subdivided into
100 four lithological zones (Ramakrishnan et al., 1998). Subsequently, based on structural and isotopic data,
101 it is reclassified into four crustal provinces with distinct evolutionary history (Dobmeier and Raith, 2003).
102 It is considered as a orogenic belt that once formed part of Proterozoic mobile belt system within the



103 Napier and Rayner complex of East Antarctica and East India (Mezer and Cosa, 1999). It is considered
104 as a segment of the global SWEAT (Southwest-United-States-East-Antarctica) orogen. Based on the
105 constituent crustal blocks, the Cuddapah basin is regarded as a collage of Proterozoic subbasins and
106 terranes (Chetty, 2001; Kale et al., 2020).

107 The basin has undergone three periods of subduction-collision related orogenic activities
108 contemporaneous with the global supercontinental episodes ~1.8 Ga (Columbia), ~1.1 Ga (Rodinia,
109 Grenvillian orogenic event), and ~550 Ma (Gondwana, East-African orogenic event) episodes as observed
110 from geochemistry and geochronological data and the presence of respective ophiolites (Mezger and
111 Cosca, 1999; Vijaya Kumar et al., 2010; Vijay Kumar and Leelanandam, 2008). This fold and thrust belt
112 thus plays an important role for the fragmentation and amalgamation of continental blocks such as those
113 of Columbia and Rodinia supercontinents (Zhao et al., 2004; Dobmeier and Raith, 2003). The CEBT is
114 formed in response to the amalgamation of the Eastern Ghats - Rayner Province terrane of East Antarctica
115 with the eastern margin of the Cuddapah basin either during the formation of the Rodinia or the Gondwana
116 supercontinent. The low-angle thrust fault, the CEBT, is especially significant as large lateral movements
117 are observed along this thrust fault. These activities make the study of the Eastern Dharwar Craton,
118 especially the structure and tectonics of the Cuddapah basin interesting and significant on a global
119 perspective of the continental crustal evolution.

120 **3. Deep crustal seismic data across the Cuddapah basin**

121 Long-range deep seismic refraction / wide-angle reflection studies were carried out along a 600
122 km long ENE-WSW trending Kavali-Udipi transect from East coast to West coast in the southern part of
123 the Indian shield (Figure 2, Profile I). Seismic data were acquired using analog instruments with typical
124 40 km shot point distance and 100 m geophone spacing using explosive as the energy source. A minimum
125 charge size of 50 kg to a maximum of 1500 kg were used for different shot-receiver distances. Thus, the
126 entire profile distance is covered by continuous profiling technique. A large number of Shot Points (SP)
127 are used to delineate the crustal structure down to the Moho and deeper (Kaila et al., 1979). The transect
128 travelled through major geological units such as the Eastern Ghats Belt, Nellore Schist Belt, Cuddapah



129 Basin, Closepet granite and Chitradurga Schist belt, thereby covering both eastern and western Dharwar
130 cratons. Deep seismic refraction / wide-angle reflection studies were also carried across the Cuddapah
131 basin, along the Alampur-Koniki profile (Figure 2, Profile II) located ~120 km north of the present
132 transect (Kaila et al, 1987).

133 The seismic data considered here for modeling the CEBT structure are recordings from the Shot
134 Points (SP) 0, 40 and 80 on the DSS Profile I across the Cuddapah basin (Figure 2). This section is part
135 of the 600 km long DSS refraction / Wide-angle reflection profile (Kaila et al., 1979), with high data
136 density and similar resolution as obtainable by reflection profiling. Deep crustal section was inferred for
137 the eastern part of the Cuddapah basin by detailed analyses of the seismic refraction / wide-angle
138 reflection data on the DSS Profile I. With the aid of a computerised method (Kaila and Krishna, 1979),
139 reversed reflection travel times data from the possible shot-point pairs were converted into the
140 corresponding reflector depth segments (covering the entire crustal section) with their reliable dips and
141 appropriate migrated positions. An initial crustal depth section assembled with those reflector segments
142 displayed the gross features of the crustal structure down to the Moho. Especially a low-angle thrust fault
143 #2 known as the Vellikonda Thrust, referred here as the CEBT, is significantly revealed to mid-crustal
144 depths. Most of the single-sided reflection arrivals data were processed by a analytical migration method
145 (Kaila et al., 1982) and those reflector segments were also included. Refraction data analysis gave some
146 details of the velocity structure, though limited to the shallow layers within the upper to mid-crustal
147 depths, with a slight indication of another low-angle fault #1. The deep crustal depth section thus inferred
148 by detailed analyses of the seismic recordings for the eastern part of the Cuddapah basin is shown in
149 Figure 3a as inferred by Kaila et al. (1979).

150 It is clear from this migrated depth section (Figure 3a) that the crustal structure in the study region
151 consists of a large number of discrete reflector segments of limited lateral extent and varying dips from
152 very shallow upper crustal depths down to the Moho and deeper. This crustal depth section looks similar
153 to the crustal reflectivity structures revealed by numerous reflection profiling experiments in various
154 regions (Mooney and Meissner, 1992; Cook, 2002). Further, since the seismic profile was chosen with its



orientation broadly perpendicular to the regional strike, the dips shown for the individual reflector segments are believed to be close to their true dips rather than being apparent. Mereu (2000) in a study on the complexity of the crust and the Moho from seismic refraction and wide-angle reflection data, considered that in the real earth reflectors are randomly located, have random velocity contrasts, and are oriented with dipping trends that have a tectonic origin. As interpreted by Kaila et al. (1979) and Roy Chowdhury and Hargraves (1981), the 600 km long crustal section across the western and eastern Dharwar cratons is divided into several individual crustal blocks by the inferred deep faults, many extending to the Moho depths, and a few thrust faults. Recently, Saikia et al. (2016) used three different approaches including, stacking, inversion, and common conversion point migration of receiver functions computed from teleseismic waveforms, recorded over seismographs located along a profile closely following the DSS profile I to understand the crustal structure. They found that the Moho depths obtained by them are in general consistent with the Moho depths in various crustal blocks bounded by the deep faults given by Kaila et al. (1979).

4. Seismic methodology for delineating complex structures

Deep seismic near-vertical reflection Profiling ("reflection profiling", with higher frequency waves or shorter wavelengths, having vertical resolution ~150 m, and horizontal resolution ~500 m) has been the most successful geophysical technique in resolving the deep structure, tectonics and evolution of the continental crust. The enhanced quality of the reflectivity images provides necessary clues for their interpretation in terms of the deep continental crustal structure and its evolution. Images of paleo-collisional and suture zones as well as detachment zones and notably the low-angle thrusts are well revealed in several studies (Mooney and Meissner, 1992). As their main characteristic, most of the images of the continental crustal structure obtained by this technique in various terranes world-wide, appear to reveal patterns of numerous discontinuous and short reflectors of varying lengths and dips as well as some regions of diffused reflectivity, even down the Moho (Cook, 2002; Mereu, 2000).

Seismic Refraction / Wide-angle Reflection Profiling ("refraction profiling", with lower frequency waves or longer wavelengths) provides complementary datasets traditionally used to derive velocity



181 structure and nature of prominent boundaries like the Moho besides other structural / physical
182 characteristics of the deep continental crust. The relatively low frequencies of seismic waves in refraction
183 profiling sample and filter the heterogeneities within the crust in a much different manner in contrast to
184 the higher frequencies of the reflection profiling experiments (Mereu, 2000). Since the longer
185 wavelengths are not suitable to resolve the smaller structures, crustal models derived from those datasets
186 especially with large spacing (1 - 2 km or more) of recorded seismic traces tend to be relatively smooth
187 and layered. Although not so common as observed by reflection profiling, high amplitude low-angle thrust
188 fault reflections are occasionally found in the field record sections acquired with favourable source-
189 receiver geometry and closer spacing of seismic traces on refraction profiles. Figures 1c and d illustrate
190 the wide-angle reflections of low-angle thrusts thus observed on a refraction profile in the southern part
191 of the Indian shield (presented here for the first time with detailed modeling) and the refraction line J of
192 the GLIMPCE experiment of the Canadian shield (Epili and Mereu, 1991). It is interesting to note from
193 these record sections that, the thrust fault reflection signature appears as prominent (with similar high
194 amplitudes and the apparent velocity) as the Moho reflection PmP phase. These typical record sections
195 are both from recordings with close spacing of the seismic traces (50-100 m) and higher frequencies like
196 the reflection profiling and unlike the traditional long-range refraction profiles with 2-5 km spacing. High
197 quality data on such refraction profiles may also reveal some unusual and high energy coherent phases
198 (Krishna and Vijaya Rao, 2011) that can be appropriately processed leading to models of crustal depth
199 sections qualitatively similar to those found by coincident reflection profiling as are being used in the
200 present study.

201 **5. A Novel modeling approach utilizing 'localized phantom horizons' and synthetic** 202 **seismograms computations**

203 Models of crustal structure inferred from seismic refraction profiles generally appear to be simple
204 with a few layers shown as apparently continuous across the model. It is difficult to derive models of both
205 velocity and the tectonic structure of complex regions as the fold belts with the available processing
206 approaches of either refraction or reflection seismic datasets. A novel modeling approach is developed
207 here to reveal the complex structures like the thrust faults and successfully applied for the first time to a



208 closely spaced refraction dataset. This approach provides crustal structure similar to near-vertical
209 reflection profiling and also the velocity structure, which is not obtainable with the conventional reflection
210 data processing technique. Detailed crustal velocity structure modeling and synthetic seismograms
211 matching of the prominent reflection signal of the inferred thrust fault were not attempted (Kaila et al.,
212 1979) earlier in their analysis of this closely spaced DSS profiling data. A recent study (Chandrakala et
213 al., 2015) in the region could neither delineate this distinct thrust fault nor recognize its reflection signal
214 on the seismograms as presented here. Their study identified a normal fault at the boundary of Nallamalai
215 Fold belt and Nellore Schist belt, instead of a thrust fault. Their findings are in contradiction with the
216 geological evidences (Saha and Tripathy, 2012; Kale et al., 2020) which suggest thrusting is responsible
217 for the formation of Nallamalai fold belt region of the Cuddapah basin. As illustrated in Figure 3a, Kaila
218 et al. (1979) have also suggested this thrusting, although its fine structure of velocity was not conclusively
219 obtained there. Thus, there is a need to refine and establish the geometry of the CEBT, and obtain a
220 plausible velocity structure in this region. These are achieved by applying our new approach to the present
221 dataset providing insight to the geodynamic evolution and imprints of the global Grenvillian and East-
222 African orogenic events in the region.

223 In order to refine and establish the geometry and structure of the significant low-angle thrust fault
224 #2 on the eastern margin of the Cuddapah basin (CEBT), and to derive a plausible velocity structure in
225 the region, we propose to use the new approach presented here. Computation of synthetic seismograms
226 compatible with the observed field record sections, especially revealing the thrust fault reflections is
227 primarily considered for this purpose. A computational technique based on the Gaussian Beam method
228 (Cerveny, 1985; Weber, 1986; Rabbel, 1987) is expressly designed for generating the synthetic
229 seismograms in the present study. We present here the digitized (Krishna and Kaila, 1986) seismic record
230 sections from SP0 and SP40 illustrating for the first-time unequivocal reflection signatures of this low-
231 angle thrust fault CEBT (Figures 5a and c).

232 Considering the migrated crustal depth section (Figure 3a) inferred by extensive data analyses
233 (Kaila et al., 1979), we generate an equivalent data set of the depth section with similar reflectivity fabric



234 but represented by a fewer reflector segments, suitable for the computational purpose. The large number
235 of smaller reflector segments in Figure 3a are replaced by a limited number of **'localized phantom**
236 **horizons'**. These are the lines drawn on the depth section such that they are parallel to as well as
237 coincident with a small group of the reflector segments thus being consistent with the local structural
238 attitude revealed in the earlier section. The large number of the actual reflector segments, which are also
239 not continuous enough to be used in the computations, are thus grouped together and replaced
240 appropriately by fewer number of localized phantom horizon segments. It should be noted here that these
241 individual localized phantom horizons created here are also of limited extent only, similar to the reflector
242 segments in the original section (Figure 3a), and in contrast to much longer phantom horizons usually
243 drawn for interpreting the seismic exploration sections. Figure 3b thus shows the recreated depth section
244 with the new localized phantom reflector horizons replacing the earlier large number of smaller reflector
245 segments. This new depth section while retaining the earlier structural fabric, it also includes all the deep
246 faults and the low-angle thrust faults as given in the original depth section for ray tracing and synthetic
247 seismogram computations.

248 Figure 3b further illustrates schematically the reflection ray paths that are generated in large
249 number for each of the reflector segments (localized phantom horizons) in the present modeling approach.
250 As shown in this schematic ray diagram, the reflected waves encounter randomly the intervening reflector
251 segments as also some of the deep faults, both in their down-going and the up-coming paths. Ray paths
252 for reflections from each of the localized phantom horizon segments are thus generated for further
253 computation of travel times and synthetic seismograms by the Gaussian Beam method. We thus consider
254 an approach in such a way, various small dipping reflectors are “embedded” in a uniform seismic velocity
255 field and the velocity increases with depth. This is in principle similar to the approach we used earlier
256 (Meru, 2000; Krishna and Vijaya Rao, 2011).

257 The earlier depth section (Figure 3a) does not give the velocity information at each of the reflector
258 segments as required for ray tracing through this complex crustal model by the approach proposed here.
259 An initial velocity model, with plausible velocity contrasts at each of the localized phantom horizon



260 segments, is developed from the earlier models (Kaila et al., 1979; Chandrakala et al., 2015; Kaila et al.,
261 1987; Chandrakala et al., 2013) in the region. The dips as well as locations of all the reflector segments
262 in the section are kept unchanged, in all the computational model input but varying only the velocity
263 contrast across each one of them to generate the reflected waves, starting from reflectors at the shallow
264 to deeper depths. The initial take-off-angles-range from the source downwards to hit a desired reflector
265 is progressively adjusted looking at the interaction of the transmitting rays with the intervening depth
266 segments until a successful hit and the reflection occurs. The final take-of-angle-ranges are fixed to let
267 interactions with all possible depth segments encountered in the up-coming paths. Thus, each of the
268 localized phantom reflector segments (a total of ~100 or more) are ray-traced and the reflection arrival
269 times are checked for possible correlations on the observed records. Any changes of the velocity contrast
270 at the reflectors are made to improve the traveltimes and synthetics fit thus generated. In the present study,
271 we intend to compute the primary reflected wave-field only, besides the refractions, to generate the
272 Gaussian Beam synthetic seismograms matching the CEBT. The same procedure can possibly be
273 extended to generate complete wavefield including other interactions like the multiples, wave-
274 conversions and diffractions but that is not considered necessary and attempted here.

275 This approach is found efficient and considered suitable for ray-tracing through, and synthetic
276 seismograms modeling of the realistic heterogeneous crustal structures consistently revealed by
277 numerous near-vertical reflection profiles as well. The crustal section considered in the present study
278 (Figure 3a) as well as its recreated version (Figure 3b) also display similarly a large number of discrete
279 reflector segments of limited lateral extent and varying dips. They are also far from being suitable for
280 approximation by a simple layered model with all the interfaces, at times hypothetically, considered to
281 exist end-to-end across the model space possibly missing the actual structural details. It was concluded
282 (Mereu, 2000) that earth models considered with sets of small randomly oriented reflectors embedded in
283 a uniform velocity gradient field will produce wide-angle reflection fields that are very similar to those
284 observed in crustal refraction experiments. The model formulation we considered here is consistent with
285 these findings. Similar conclusions were also made earlier (Long et al., 1994), suggesting that nature of
286 both reflection and refraction profiling data sets has a common cause relating to the basic structure of the



crust and in particular to the discontinuous nature of crustal reflectors. Those reflectors are modelled as local velocity variations rather than part of large-scale velocity change laterally or vertically. It was also opined (Long et al., 1994) that the crustal models that show existence of velocity discontinuities extending over large distances, as traditionally inferred from refraction profiles, are questionable. The present modeling approach is specifically developed for synthesizing the wide-angle reflection wave-field for the heterogeneous crustal structure consisting of large number of discontinuous reflectors and the low-angle thrust fault which is the major target in the study region (Figures 3a, b).

294

295 **6. Tectonic imbrication of Proterozoic accretions**

The modeling approach developed and used here adequately considers the discontinuous nature of the continental crustal structure consisting of several small and distinct reflector segments clearly revealed in the earlier crustal depth section (Kaila et al., 1979). Such a nature of the continental crustal structure, as also considered earlier (Mereu, 2000; Long et al., 1994) to be more realistic, is consistently supported in several deep seismic reflection profiling experiments in a variety of tectonic regions in the world (Cook, 2002; Mooney and Meissner, 1992). The new modeling approach is used for successful ray-tracings from the CEBT with its fine structure from SP0, SP40 and SP80 as illustrated in Figures 4(a, b and c). Following the ray tracings for the undisturbed structural model as in Figure 3b, and iterating and inferring of the velocities across in the process for all the localized phantom reflector segments, the synthetic seismograms are generated as shown Figures 5 b and d. Especially, the reflections of the low-angle thrust-fault, generated in the synthetics are quite consistent with those found in the observed record sections (Figures 5a and c), thus confirming its geometry (including some inferred layering within) displaying a high velocity (6.8 - 7.3 km/s) structure for it. Thus, it is evident that the CEBT is characterized with a high velocity, and possibly a high-Q (low absorption) structure as well. The P wave velocity structure of the crust and geometry of the thrust-fault is presented in Figure 6a. These structural properties of the CEBT are obtained here for the first time by the new modeling approach developed here. The CEBT is significantly revealed in the seismic record sections of SP0 and SP40 (up-dip recording, as shown here) and it is also seen in record section of SP80 (down-dip recording) on the eastern margin of



314 the Cuddapah basin. A similar low-angle thrust fault (like the CEBT) on the eastern margin of the basin
315 was found (Kaila et al., 1987) also on the profile II located ~120 km north of profile I (Figure 2). The
316 CEBT is thus considered as a major tectonic feature of the Cuddapah basin. The CEBT with a stack of
317 reflectors (Figure 6a) is similar to the thrust faults imaged in the deep crustal seismic reflection profiling
318 studies as shown in Figures 1(a, b).

319 The CEBT demarcates distinctly different velocity structure, lithology and metamorphism
320 (greenschist on the west and granulites on the east) as also reported (Dobmeier and Raith, 2003) earlier.
321 Eastward dipping geometry of the thrust fault suggests that the Dharwar craton subducted to the east and
322 the eastern crustal block was up-thrust to the west. Presence of the Kanigiri ophiolitic mélange
323 (DharmaRao et al., 2011) (~1.3 Ga) in the northern part of the CEBT (Figure 2) suggests presence of an
324 ocean and associated subduction zone in the region during early Neoproterozoic. Further, the geological
325 and geochemical data indicate that the Nellore Schist Belt represents the upper crustal segments of a
326 subduction zone associated with island arc development and closure (Kale et al., 2020; Vijaya Kumar and
327 Leelanandam, 2008; Dharma Rao, et al., 2011; Saha and Sain, 2019). Most of the crustal reflectors from
328 shallow depths to the Moho boundary of the Nallamalai Fold belt domain show consistent eastward dip
329 from SP140 to the CEBT (Figures 3a and b and 6a). These east-dipping reflectors change the dip direction
330 to the west from the CEBT (Figure 6a). These east-west dipping reflectors constitute a bivergent reflection
331 fabric that represents the signature of a collision zone (BABEL Working Group, 1990; Hall and Quinlan,
332 1994; Vijaya Rao et al., 2000). The uniqueness of the present study is identification of bivergent
333 reflections from DSS refraction / reflection dataset. These bivergent reflections characterize different
334 crustal blocks on either side of the boundary. The collision process has resulted in crustal shortening and
335 thickening as observed from the thickest crust at the CEBT boundary (Figure 6a). Crustal velocities in
336 the upper and middle crust of the NFB are 0.2 km/s greater than those normally found in shield regions.
337 This could be a result of collision which has pushed the deeper rocks towards the surface during the
338 orogenic activity. Similar high velocities are observed from several other orogenic belts, e.g. the Grenville
339 region (Mereu, 2000).



340 Beneath the eastern part of Cuddapah basin, the CEBT, Kaila et al. (1979) identified two
341 prominent reflector bands in the deeper part of the crust, one at 40 km and another at 45 km depth (Figure
342 3a). They referred them as a double Moho-discontinuity. Subsequently, Kaila and Sain (1997) have
343 suggested 42 km thick crust beneath the CEBT. Reanalysis of seismic refraction data using ray methods
344 suggests 47 km thick crust at the CEBT, the Nallamalai Fold Belt-Nellore Schist Belt boundary
345 (Chandrakala et al., 2015). The present study using the Gaussian beam technique has identified the Moho
346 at a depth of ~45 km, which is consistent with the deeper Moho boundary delineated by Kaila et al.
347 (1979). The present results are in conformity with the global compilation study that suggests thicker crust
348 of the order of ~45 km for the Proterozoic and thinner for the Archean regions (Durrheim and Mooney,
349 1991). A crustal thickness of 47 km was imaged for the Proterozoic Aravalli-Delhi Fold Belt region of
350 NW India (Vijaya Rao et al, 2000; Krishna and Vijaya Rao, 2011). Geological studies also suggest 45-50
351 km thick crust at the CEBT (Dobmeier and Raith, 2003; Saha and Tripathy, 2019). Thick crust in the
352 region could be due to collisional activity and subsequent magmatic underplating observed in the region
353 (Kaila and Sain, 1997; Chandrakala et al., 2015). Large dyke swarm activities at 1.8 and 1.1 Ga (French
354 et al., 2008; Kumar et al., 1993) observed in the region are manifestations of crust-mantle interaction
355 process that resulted in magmatic underplating. However, the receiver function study identified the Moho
356 at 40 km depth.

357 Bouguer gravity anomaly map of the region reveals prominent steep gravity increase of ~60
358 mGals within a 50 km distance, across the collisional boundary (Figure 3a). This gravity anomaly is a
359 regional feature extending all along this 350 km long boundary (NGRI, 1978), and is significant to
360 providing insight for the tectonic evolution of the region. Observations of steep gradient bipolar (low-
361 high pair) gravity anomaly across the CEBT, suggests that this boundary can be a faulted contact of
362 juxtaposed crustal blocks. It is consistent with the gravity high observed over the thrust fault. The gravity
363 low corresponds to the under-thrust block while the gravity high characterises the over-thrust crustal
364 block. This is consistent with the observed seismic signature modelled here as the low-angle thrust fault.
365 Gravity studies from the Canadian, Australian, Indian and other shield regions suggest that a steep



366 gradient bipolar gravity anomaly is a characteristic signature of a suture (Gibb and Thomas, 1976;
367 Fountain and Salisbury, 1981; Vijaya Rao et al., 2000; Singh and Mishra, 2002).

368 Arcuate-basin-pattern and convex-to-the-west thrust eastern margin of the Cuddapah basin, 'the
369 Cuddapah salient', also indicates east-west convergence and operation of collision tectonics in the region.
370 Based on the seismic reflection signature of the thrust fault and the available geological data, we interpret
371 that subduction and collision are responsible for the crustal evolution and the CEBT in the region. The
372 collision took place between the Dharwar craton in the west and the Nellore Schist Belt-Eastern Ghats
373 Belt-Rayner complex of east Antarctica, a combined continental block to the east forming an extensive
374 orogenic belt contemporaneous with the global Grenvillian orogenic activity at ~1.0 Ga. Earlier
375 geological studies have identified a collision during this period at this boundary (Mezger and Cosa, 1999;
376 Vijaya Kumar and Leelanandam, 2008).

377 The geodynamic evolutionary scenario displayed by the seismic structure and consistent with the
378 geological data are presented in the form of a schematic model in Figure 6b. It shows two crustal blocks
379 separated by an ocean and subsequently the western block consisting of the Eastern Dharwar Craton and
380 Cuddapah basin subducted to the east and collided with the Nellore Schist Belt-Eastern Ghats Belt-Rayner
381 complex (eastern Block). The low-angle thrust-fault, CEBT formed during this collisional episode on the
382 eastern margin of the Cuddapah basin acts as a suture by juxtaposing two crustal blocks of different
383 physical properties and evolutionary histories. The collisional activity observed in the region is a marginal
384 segment of a larger orogenic belt during late Proterozoic and related to the assembly of the Rodinia
385 supercontinent (Hoffman 1991; Mezger and Cosca, 1999). Relict-suture zones were identified (Burke et
386 al., 2003) in Africa based on the deformed alkaline rocks and carbonatites. Similar studies have identified
387 the CEBT as a paleo-collision and suture zone (Leelanandam et al., 2006).

388 Lower elevation in the collision zone (Figure 2) indicates orogenic collapse and operation of post-
389 collisional extensional processes, which might have emplaced several alkaline-granitoid bodies in the
390 region. The high-velocity (6.8 - 7.3 km/s) bodies along the thrust (Figure 6a) indicate such intrusives,
391 namely anorthosites, carbonatites and ophiolitic mélangé. The CEBT acted as a channel for the



392 transportation of enriched mineralized fluids from the upper mantle depth to the surface and responsible
393 for the mineralization of the Cuddapah basin, which is recognized as one of the richest mineralized zones
394 in India. The East Gondwana fragments, namely India, Antarctica, Australia and South Africa were
395 amalgamated along the Circum-East Antarctic mobile belts during the assembly of early Neoproterozoic
396 Rodinia supercontinent (Hoffman, 1991). These crustal blocks were reworked during the late
397 Neoproterozoic-early Cambrian East-African orogenic (~550 Ma) activity symbolizing the accretion of
398 East and West Gondwanas with the formation of the Gondwana supercontinent. Based on the later
399 activity, it was suggested (Dobmeier et al., 2006) that the combined Eastern Ghats Belt-Rayner Complex
400 accreted to the Dharwar craton during the East-African orogenic episode.

401 The present study identified another low-angle thrust fault # 1 extending from the surface to a
402 depth of 20 km to the east of CEBT. It separates distinct geological terranes, namely the Nellore Schist
403 Belt and Eastern Ghats Belt. Similar low-angle thrust fault was also delineated (Kaila et al., 1987) along
404 the seismic profile II, located ~120 km to the north of present transect (Figure 2). It is also located at the
405 eastern margin of Nellore Schist Belt. Thus, the dipping feature can be regarded as a regional feature. The
406 significance of this feature (fault # 1) was not discussed in any one of the earlier works (Kaila et al., 1987;
407 Chandrakala et al., 2013, 2015). Presence of 1.9 Ga Kandra ophiolitic complex representing dismembered
408 Paleoproterozoic supra-subduction zone ophiolite (Vijaya Kumar et al., 2010) at this thrust fault region
409 indicates presence of oceanic crust during late Paleoproterozoic period (Figure 2). We interpret
410 subduction of oceanic crust and collision between the Nellore Schist Belt and another crustal block to the
411 east (Probably East Antarctica) has resulted in the development of Eastern Ghats orogen with the
412 formation of a thrust fault between them. Generally, mountain belts represent regions where oceans might
413 have opened and closed and they are the products of continental collision (Dewey and Bird, 1970). We
414 refer this thrust fault as the Eastern Ghats Thrust (EGT). During the Late Paleoproterozoic period various
415 continental blocks from different parts of the world, including the Eastern Ghats Belt of India were
416 involved in the process of accretion and formation of Columbia supercontinent by subduction and
417 collision processes (Rogers and Santosh, 2002; Vijaya Rao and Reddy, 2002; Vijaya Kumar et al., 2011).
418 The compressional forces developed during this period might also be responsible for the thrusting,



419 collision and formation of Eastern Ghats Belt over this part of the Indian shield. Several geological,
420 geochemical and geochronological studies have suggested the formation of Eastern Ghats Belt during
421 ~1.8 Ga due to subduction and collision between eastern part of the Dharwar craton and probably Rayner
422 complex of East Antarctica (Vijaya Kumar and Leelanandam, 2008; Vijaya Kumar et al., 2010; Dasgupta
423 et al., 2013; Saha and Sain, 2019). The suggested evolutionary model of the region is illustrated in figure
424 6b.

425 Seismic structure derived from the present study provides basic constraints for proper correlation
426 of Gondwana fragments and supercontinental formation. It also provides mechanism for the
427 mineralization of the region and crustal evolution during the Proterozoic. Integrating the crustal structure,
428 inferred seismic velocity model specifically of the CEBT, steep gradient bipolar gravity anomaly,
429 presence of the alkaline and carbonatite rocks, geochemical signatures representing the island-arc,
430 subduction zone environment (Vijaya Kumar and Leelanandam, 2008; Kale et al., 2020; Saha and Sain,
431 2019) and anorthosites, the EGT and CEBT are interpreted as relict subduction-collisional suture evolved
432 during the Late Paleo- and Mesoproterozoic Proterozoic periods.

433 7. Conclusions

- 434 • A new approach is developed for modeling crustal depth sections revealing several limited extent
435 discrete reflector segments in the refraction profiling data. These reflectors are modelled as local
436 velocity variations, and not necessarily part of large-scale velocity changes. The crustal structure
437 derived from this approach closely resembles the images obtained by reflection profiling data as
438 well, closer to the real Earth models. **Localized phantom horizons** approach of refraction data
439 developed here is more useful in understanding the tectonic evolution of the regions of complex
440 tectonic origin compared to conventional layered models inferred by other methods.
- 441 • Closely spaced (50-100 m) refraction datasets can be used to delineate both the velocity structure
442 and geometry of the thrust fault regions by this approach as shown in this study.
- 443 • Conventional simple layered modeling approach of refraction data, where velocity discontinuities
444 are often assumed to extend over a large distances, is likely to miss the fine structural details.



445 • Present study suggests the NSB is sandwiched between the EGB toward the east and the Dharwar
446 Craton toward the west during the Late Paleo- and Mesoproterozoic collisional activities resulting
447 in the formation of the EGT and CEBT.
448 These events are contemporaneous with the global Columbia and Rodinia or East-African
449 supercontinental episodes.

450

451 **Acknowledgements**

452 The seismic data presented here was acquired by the CSIR - National Geophysical Research Institute,
453 Hyderabad-500007, India, as part of the Deep Seismic Sounding Project. We gratefully acknowledge the
454 project scientists, technical personnel, and the Director, CSIR - National Geophysical Research Institute.
455 We thank K. Laxminarayana and Karuppannan for a few figure tracings.

456 **Contributions**

457 V.G.K. designed the study, contributed the methodology development and modelled the seismic data.
458 V.G.K. and V.V.R. interpreted the seismic results proposing a plausible geodynamic evolutionary model
459 consistent with the seismic results. V.V.R. examined additional inputs for correlation with the geological
460 data.

461 **Ethics declarations**

462 **Competing interests**

463 The authors declare no competing interests.

464 **References**

465 BABEL Working Group.: Evidence for early Proterozoic plate tectonics from seismic reflection profiles
466 in the Baltic Shield. *Nature*, 34, 34-38, 1990.



- 467 Burke, K., Ashwal, L.D. and Webb, S.J.: New way to map old sutures using deformed alkaline rocks and
468 carbonatites. *Geology*, 31, 391–394, 2003.
- 469 Cervený, V. Gaussian beam synthetic seismograms.: *J. Geophys.*, 58, 44-72, 1985.
- 470 Chetty, T.R.K., (2001). The Eastern Ghats Mobile Belt, India: A collage of juxtaposed terranes.:
471 *Gondwana Research*, 4, 319-328.
- 472 Chandrakala, K., Pandey, O.P., Prasad, A.S.S.R.S. and Sain, K.: Seismic imaging across the Eastern
473 Ghats Belt-Cuddapah Basin collisional zone, southern Indian Shield and possible geodynamic
474 implications. *Precam. Res.*, 271, 56-64, 2015.
- 475 Chandrakala, K., Mall, D.M., Sarkar, D. and Pandey, O.P. (2013). Seismic imaging of the Proterozoic
476 Cuddapah basin, south India and regional geodynamics. *Precam. Res.*, 231, 277-289, 2013.
- 477 Cook, F.A.: Fine structure of the continental reflection Moho. *GSA Bull.*, 114, 64-79, 2002.
- 478 Dewey, J.F., Bird, J.M.: Mountain belts and new global tectonics. *J Geophys Res* 75:2625–2647, 1970.
- 479 Dharma Rao, C.V., Santosh, M. and Yuan-Bao, W.: Mesoproterozoic ophiolitic mélangé from the SE
480 periphery of the Indian plate: U–Pb zircon ages and tectonic implications. *Gondwana Res.*, 19, 384 -
481 401, 2011.
- 482 Dobmeier, C, and Raith, M.: Crustal architecture and evolution of the Eastern Ghats Belt and adjacent
483 regions of India. *Geological Society of London, Spec. Pub.*, 206, 145–168, 2003.
- 484 Dobmeier, C, Lutke, S, Hammerschmid, K. and Mezger, K.: Emplacement and deformation of the
485 Vinukonda meta-granite (Eastern Ghats, India) - Implications for the geological evolution of
486 peninsular India and for Rodinia reconstructions. *Precamb. Res.*, 146, 165-178, 2006.
- 487 Durrheim, R.J., and Mooney, W.D.: Archean and Proterozoic crustal evolution: Evidence from crustal
488 seismology. *Geology*, 19, 606-609, 1991.
- 489 Epili, D. and Mereu, R.F.: The Grenville Front tectonic zone: Results from the 1986 Great Lakes onshore
490 seismic wide-angle reflection and refraction experiment. *J. Geophys. Res.*, 96, 16,335-16,348, 1991.
- 491 Fountain, D.M. and Salisbury, M.H.: Exposed cross-sections through the continental crust: implications
492 for crustal structure, petrology, and evolution. *Earth Planet. Sci. Lett.*, 56, 263–277, 1981.



- 493 Gibb, R.A. and Thomas, M.D.: Gravity signature of fossil plate boundaries in the Canadian Shield. *Nature*,
494 262, 199–200, 1976.
- 495 Hall, J. and Quinlan, G.: A collisional crustal fabric pattern recognised from seismic reflection profiles of
496 the Appalachian / Caledonide orogen. *Tectonophysics*, 232, 31–42, 1994.
- 497 Hoffman, P.F.: Did the Breakout of Laurentia Turn Gondwanaland Inside-Out? *Science*, 252, 1409–1412,
498 1991.
- 499 Kale, V.S., Saha, D., Deb, S.P., Sesha Sai, V.V., Tripathy, V. and Patil-Pillai, S.: Cuddapah Basin, India:
500 a collage of Proterozoic subbasins and terranes. *Proc. Indian Natn. Sci. Acad.*, 86, 137–166, 2020.
- 501 Kaila, K.L., Roy Chowdhury, K., Reddy, P.R., Krishna, V.G., Hari Narain, Subbotin, S.I., Sollogub, V.B.,
502 Chekunov, A.V., Kharetko, G.E., Lazarenko, M.A., and Ilchenko, T.V. Crustal structure along
503 Kavali-Udipi profile in the Indian peninsular shield from deep seismic sounding. *J. Geol. Soc. India*,
504 20, 307–333, 1979.
- 505 Kaila, K.L. and Krishna, V.G.: A new computerised method for finding effective velocity from reversed
506 reflection travel time data. *Geophysics*, 44, 1064–1076, 1979.
- 507 Kaila, K.L., Roy Chowdhury, K., and Krishna, V.G.: An analytical migration method for crustal wide-
508 angle reflections. *Studiageophysica et geodaetica.*, 26, 254–271, 1982.
- 509 Kaila, K.L., Tewari, H.C., Roy Chowdhury, K., Rao, V.K., Sridhar, A.R. and Mall, D.M.: Crustal
510 structure of the northern part of the Proterozoic Cuddapah basin of India from deep seismic soundings
511 and gravity data. *Tectonophysics*, 140, 1–12, 1987.
- 512 Krishna, V.G. and Kaila, K.L.: Digitization of analog DSS records and their reinterpretation with the aid
513 of synthetic seismograms - application to Koyna data. in: Deep Seismic Soundings and Crustal
514 Tectonics, Eds. K.L. Kaila, and H.C. Tewari, AEG Publ., 99–119, 1986.
- 515 Krishna, V.G. and Vijaya Rao, V.: Velocity modeling of a complex deep crustal structure across the Meso-
516 Proterozoic south Delhi fold belt, NW India, from joint interpretation of coincident seismic wide-
517 angle and near-offset reflection data – An approach by utilizing unusual reflections in wide-angle
518 records. *J. Geophys. Res.*, **116**, B01307, doi: 10.1029/2009JB006660, 2011.



- 519 Kumar, A., Padma Kumari, V.M., Dayal, A.M., Murthy, D.S.N. and Gopalan, K.: Rb-Sr ages of
520 Proterozoic kimberlites of India, evidence for contemporaneous emplacement. *Precambrian*
521 *Research*, 62, 227-237, 1993.
- 522 Leelanandam, C., Burke, K., Ashwal, L.D. and Webb, S.J.: Proterozoic mountain building in Peninsular
523 India: an analysis based primarily on alkaline rock distribution. *Geological Magazine*, **143**, 195–212,
524 2006.
- 525 Long, R.E., Matthews, P.A. and Graham, D.P.: The nature of crustal boundaries: combined interpretation
526 of wide-angle and normal-incidence seismic data. *Tectonophysics*, 232, 309-318, 1994.
- 527 Mandal, B., Sen, M.K., Vijaya Rao, V. and Juergen Mann.: Deep seismic image enhancement with the
528 common reflection surface (CRS) stack method: evidence from the Aravalli–Delhi fold belt of
529 northwestern India. *Geophys. J. Int.*, 196, 902-917, 2014.
- 530 Mezger, K. and Cosca, M.A.: The thermal history of the Eastern Ghats Belt (India) as revealed by U–Pb
531 and $^{40}\text{Ar}/^{39}\text{Ar}$ dating of metamorphic and magmatic minerals: implications for the SWEAT
532 correlation. *Precamb.Res.*, 94, 251-271, 1999.
- 533 Mereu, R.F.: The complexity of the crust and Moho under the southeastern Superior and Grenville
534 provinces of the Canadian Shield from seismic refraction – wide-angle reflection data. *Can. J. Earth*
535 *Sci.*, 37, 439-458, 2000.
- 536 Mooney, W.D. and Meissner, R.: In *Continental Lower Crust* (eds. D.M.Fountain, R.Arculus, and
537 R.W.Kay) 45-79 Elsevier, Amsterdam., 1992.
- 538 N.G.R.I. NGRI/GHP-1 to 5: (1978). Gravity Maps of India. Scale 1:5,000,000. National Geophysical
539 Research Institute, Hyderabad, India.
- 540 Rabbel,W.: Seismische Erkundung oberflaechennaher Stoerzonen: Strahlen-theoretische Grundlagen
541 und Feld beispiele, Ph.D. thesis, Univ. of Kiel, Kiel, Germany., 1987.
- 542 Ramakrishnan, M., Nanda, J.K. and Augustine, P.F.: Geological evolution of the Proterozoic Eastern
543 Ghats MobileBelt. *Geol. Surv. Spec. Publ.* No.44, 1-21, 1998.
- 544 .Ramam, P.K., Murthy, V.N.: Geology of Andhra Pradesh. Geol. Soc. India,Bangalore, 245p., 1997.



- 545 Ravikant, V.: Paleoproterozoic (~1.9 Ga) extension and breakup along the eastern margin of the Eastern
546 Dharwar Craton, SE India: New Sm–Nd isochron age constraints from anorogenic mafic
547 magmatism in the Neoarchean Nellore greenstone belt. *Journal of Asian Earth Sciences*, 37, 67–81,
548 2010.
- 549 Rogers, J.J.W. and Santosh, M.: Configuration of Columbia, a Mesoproterozoic supercontinent.
550 *Gondwana Res.*, 5, 5–22, 2002.
- 551 Roy Chowdhury, K. and Hargraves, R.B.: Deep seismic soundings in India and the origin of continental
552 crust. *Nature*, 291, 648–650, 1981.
- 553 Saha, D. and Tripathy, V.: in *Paleoproterozoic of India Spec. Pub. 365* (eds. R. Mazumder and D. Saha)
554 161–184 Geological Society, London., 2012.
- 555 Saikia, U., Rai, S.S., Meena, R., Prasad, B.N.V. and Borah, K.: Moho offsets beneath the Western Ghat
556 and the contact of Archean crusts of Dharwar Craton, India. *Tectonophysics*, 672–673, 177–189, 2016.
- 557 Saha, D. and Sain, A.: Multiple granites and granulite domains along the SE margin of India. *Journal of*
558 *Geodynamics*, 129, 44–58, 2019.
- 559 Singh, A.P. and Mishra, D.C.: Tectono-sedimentary evolution of Cuddapah basin and Eastern Ghats
560 mobile belt (India) as Proterozoic collision: gravity, seismic and geodynamic constraints. *J.*
561 *Geodynamics*, 33, 249–267, 2002.
- 562 Vijaya Kumar, K., Ernst, W.G., Leelanandam, C., Wooden, J.L. and Grove, M.J.: First Paleoproterozoic
563 ophiolite from Gondwana: Geochronologic–geochemical documentation of ancient oceanic crust
564 from Kandra, SE India. *Tectonophysics*, 487, 22–32, 2010.
- 565 Vijaya Kumar, K., and Leelanandam, C.: Evolution of the Eastern Ghats Belt, India: a plate tectonic
566 perspective. *J. Geol. Soc. India*, 72, 720–749, 2008.
- 567 Vijaya Kumar, K., Leelanandam, C., Ernst, W.G.: Formation and fragmentation of the Palaeoproterozoic
568 supercontinent Columbia: evidence from the Eastern Ghats Granulite Belt, southeast India. *Int.*
569 *Geol. Rev.* 53, 1297–1311, 2011.



- 570 Vijaya Rao, V., Rajendra Prasad, B., Reddy, P.R. and Tewari, H.C.: Evolution of Proterozoic Aravalli
571 Delhi fold belt in the northwestern Indian shield from seismic studies. *Tectonophysics*, 327, 109-130,
572 2000.
- 573 Vijaya Rao V., Reddy P.R.: A Mesoproterozoic supercontinent: evidence from the Indian Shield. In:
574 Rogers JJW, Santosh M (eds.) Special volume on Mesoproterozoic supercontinent, *Gondwana*
575 *Research*, 5:63–74, 2002.
- 576 Vijaya Rao, V.: In *Geodynamics of the Collision Zone*. J. Geol. Soc. India Memoir 72 (eds. B.R. Arora
577 and Rajesh Sharma) 165-194, *J. Geol. Soc. India*, Bengaluru., 2009.
- 578 Weber, M.: Die Gauss-Beam Methode zur Berechnung theoretischer Seismogramme in absorbierenden
579 inhomogenen Medien: Test und Anwendung, Ph.D. thesis, Univ. of Frankfurt, Frankfurt, Germany.,
580 1986.
- 581



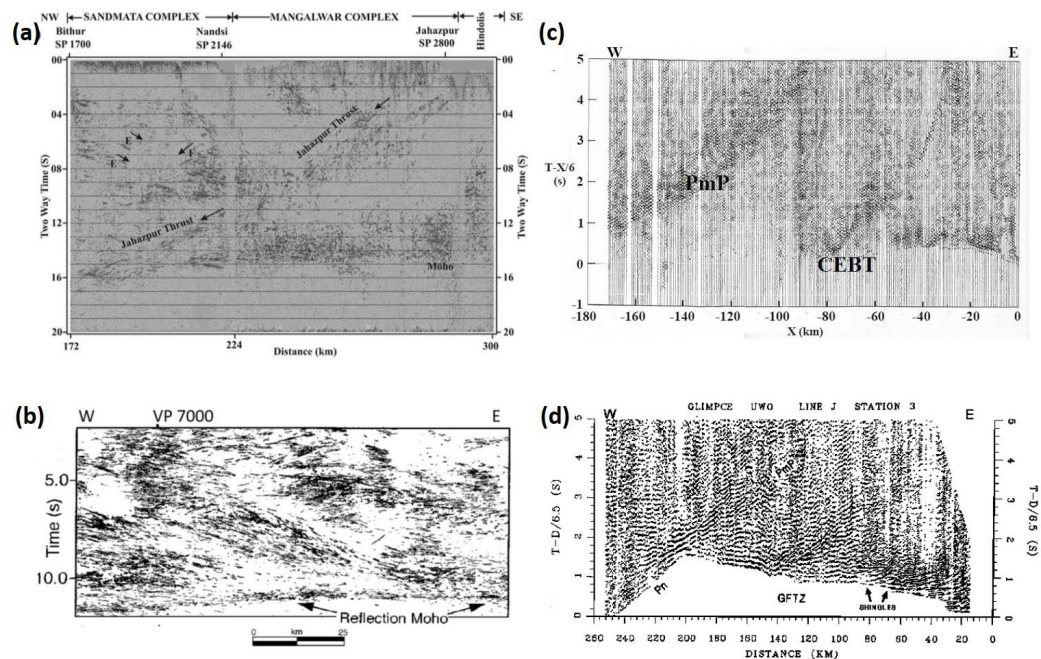
582

583 **Table-1: Tectonic framework of Eastern Dharwar Craton**

2.7-2.9 Ga	: Peninsular Gneisses
2.7-2.55 Ga	: Formation of a large number of linear Greenstone (schist) belts
2.5 Ga	: Accretion of western and eastern Dharwar cratons. Wide-spread calc-alkaline to potassic granites
2.3-2.1Ga	: Mafic dyke swarms
1.8 Ga	: Mafic magmatism -formation of Paleoproterozoic Large Igneous Province (French et al., 2000)
1.8-0.8Ga	: Formation of the Proterozoic Cuddapah, Kaladgi and Bhima basins
1.8 Ga	: Collision between the EDC and Antarctica and formation of Eastern Ghats Orogenic belt. Formation of Granulites.
1.1 Ga	: Collision between EDC & NSB (Nellore Schist Belt)-EGMB continental block with the formation of Nallamalai foldbelt. Kimberlite Volcanism (Kumar et al., 1993). Alkaline magmatism (Carbonatites) and anorthosites
550 Ma	: East-African Orogeny related to formation of Gondwana Supercontinent (Dobmeier and Raith, 2003; Meert, 2003; Yoshida et al., 2003).
118 Ma	: Separation of Australia-Antarctica from the east coast. Evolution of Rajmahal traps and formation of Indian ocean.
90 Ma	: Kimberlite Volcanism

584

585



586

587 **Figures 1 a, b.** Typical images of prominent thrust faults delineated on seismic reflection profiles. (a)
588 Jahazpur thrust evolved during the Paleoproterozoic Aravalli orogen of the NW part of the Indian shield
589 (Mandal et. al., 2014), (b) Great Bear arc related to the Wopmay orogen of the Canadian shield (Cook,
590 2002).

591 **Figures 1 c, d.** Significant wide-angle reflection images from the thrust faults observed on a few specific
592 favourably oriented refraction profiles. (c) illustrates the reflection data modelled and interpreted here,
593 (d) illustrates the reflection data across Grenvillian Front Tectonic Zone, GFTZ (Epili and Mereu, 1991).

594

595

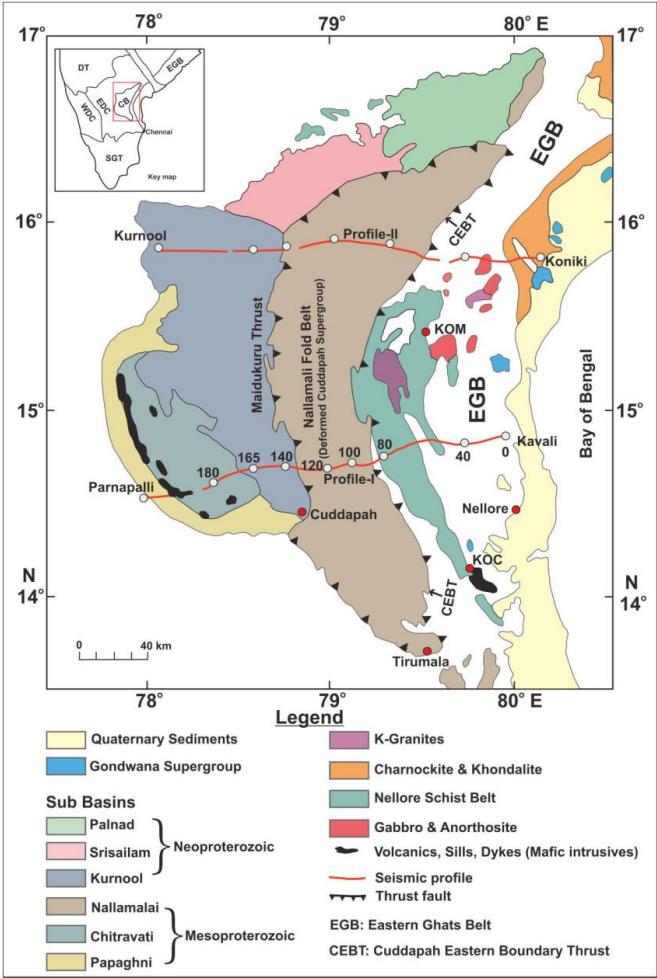
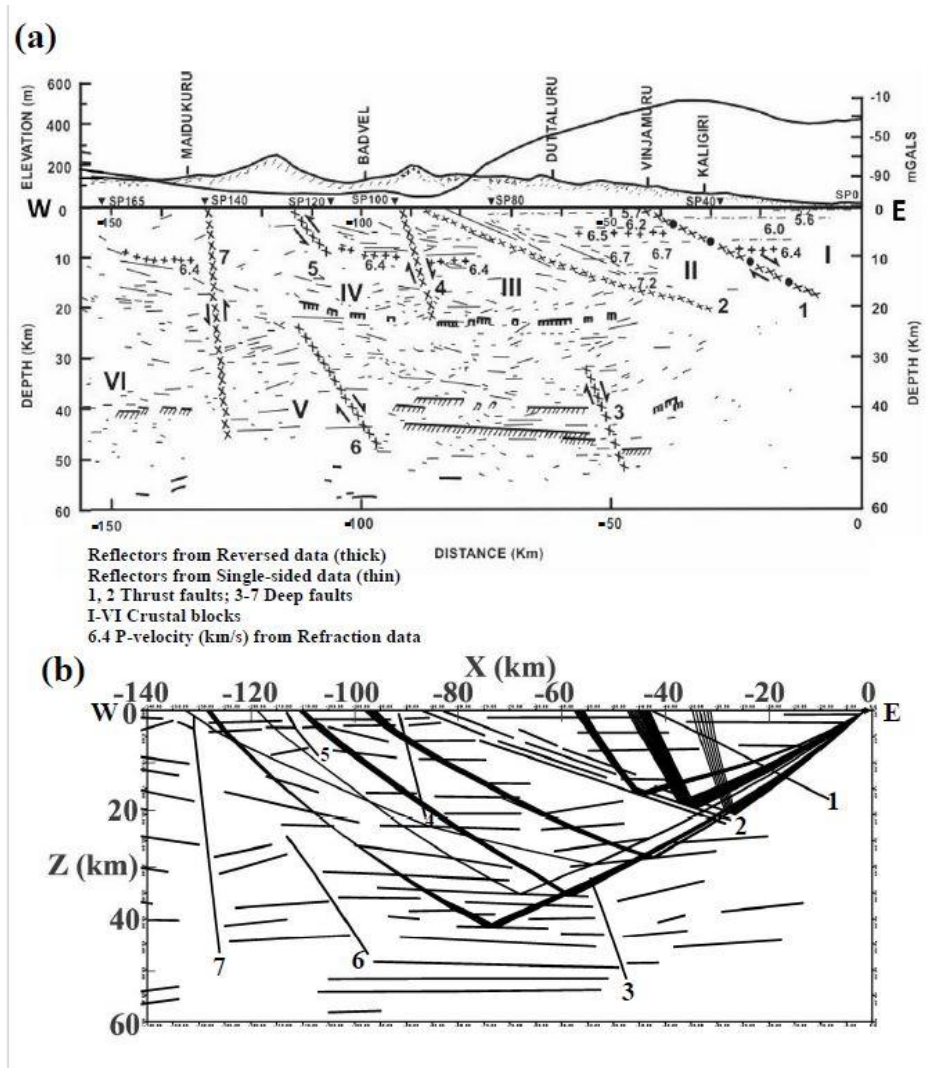


Figure 2. Geological map of the Cuddapah basin (modified after Ramam and Murthy, 1987) showing the distribution of different sub-basins. Locations of the two DSS profiles I and II across the basin. The present study uses the observations from SP0, SP40 and SP80 on the eastern part of the Profile I. NFB: Nallamalai Fold Belt, EGMB: Eastern Ghats Mobile Belt, KOM (Kanigiri) and KOC (Kandra) are the locations of ~1.9 Ga and 1.8 Ga ophiolites. Key map shows the location of the Cuddapah Basin (CB) in the EDC (Eastern Dharwar Craton) and relative to the WDC (Western Dharwar Craton). 0, 40, 80, 100, 120, 140, 165, 180 indicate various shot points operated on the Profile I.



604

605 **Figure 3a.** Deep crustal section inferred (Kaila et. al., 1979) for the eastern part of the Cuddapah basin
606 by detailed analyses of the seismic refraction / wide-angle reflection data on the DSS Profile I. The 600
607 km long crustal section across the EDC through the WDC is divided into several individual crustal blocks
608 (Kaila et. al., 1979; Roy Chowdhury and Hargraves, 1981) by the inferred deep faults, many extending
609 to the Moho depths, and a few thrust faults.

610 **Figure 3b.** An equivalent data set of the crustal section with similar reflectivity fabric represented by
611 fewer reflector segments, suitable for the computational purpose. The large number of smaller reflector
612 segments in Figure 3a are replaced by a limited number of 'localized phantom horizons'. Reflection ray



613 paths that are generated in large number for each of the localized phantom reflector segments (a total of
614 ~100 or more) in the present modeling approach are also illustrated schematically. As shown here, the
615 reflected waves encounter randomly the intervening reflector segments as also some of the deep faults,
616 both in their down-going and the up-coming paths.

617

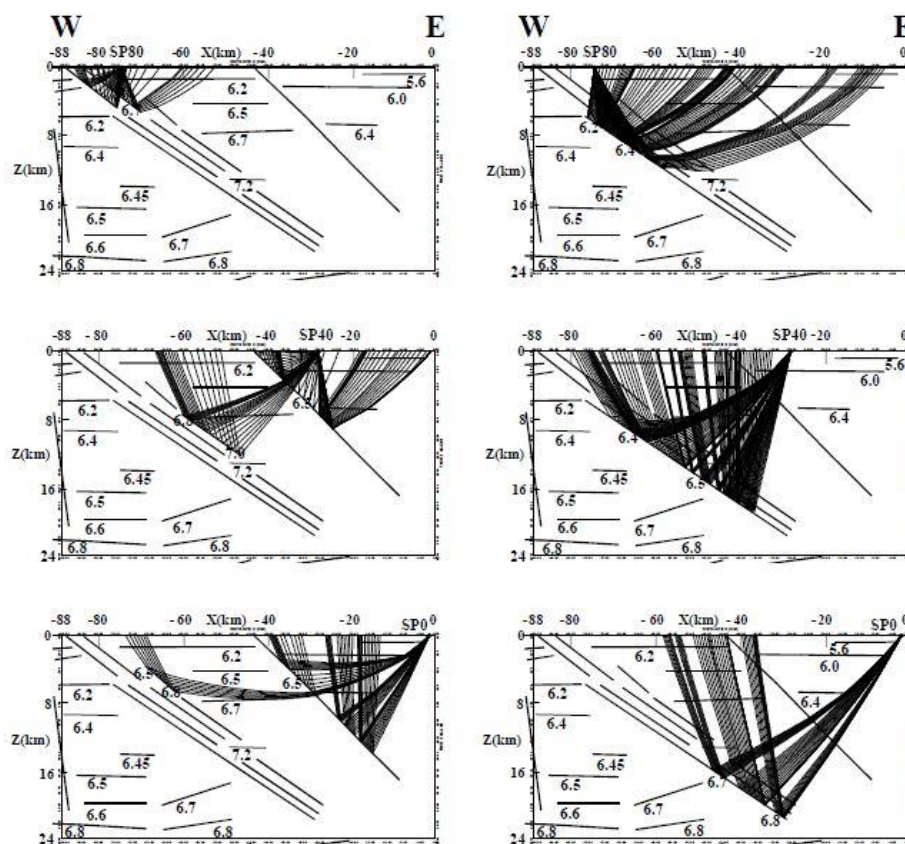


Figure 4a

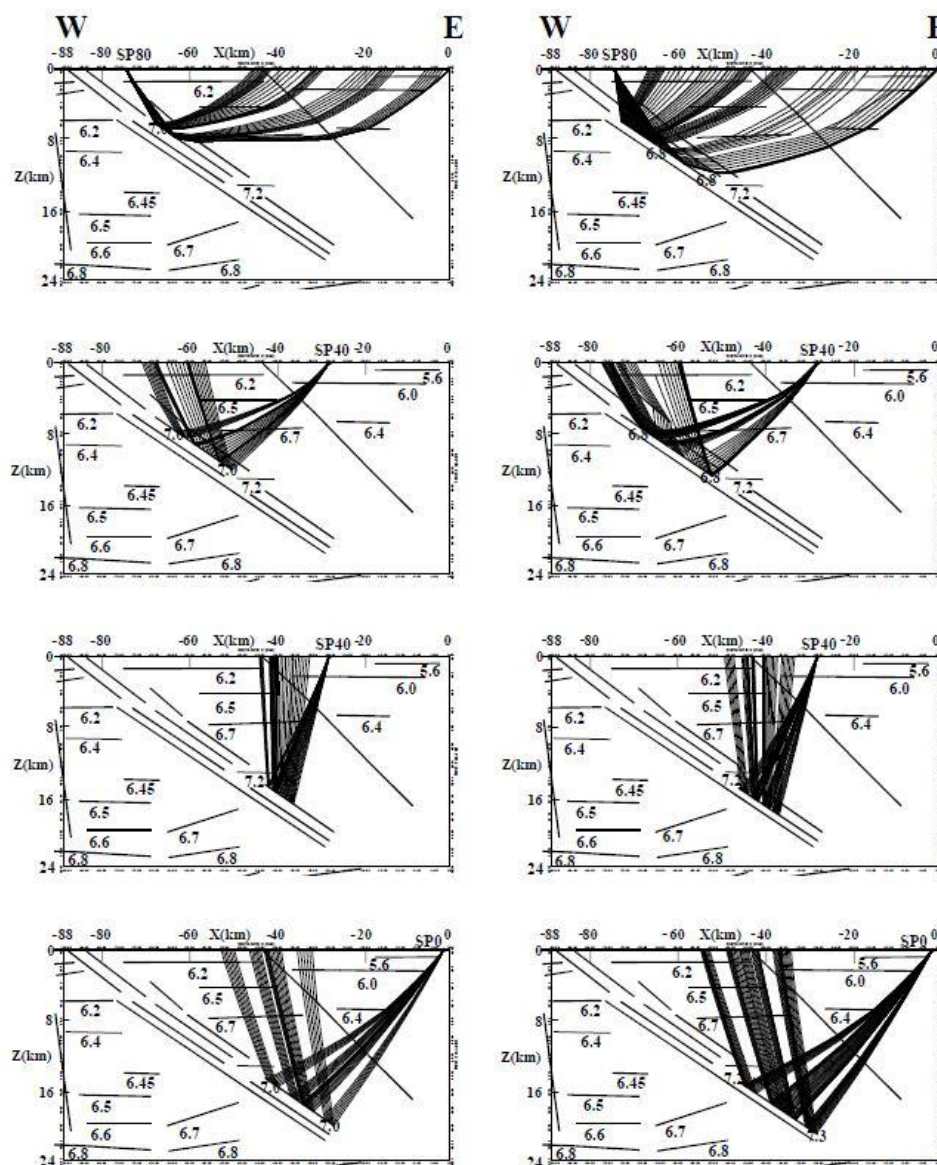


Figure 4b

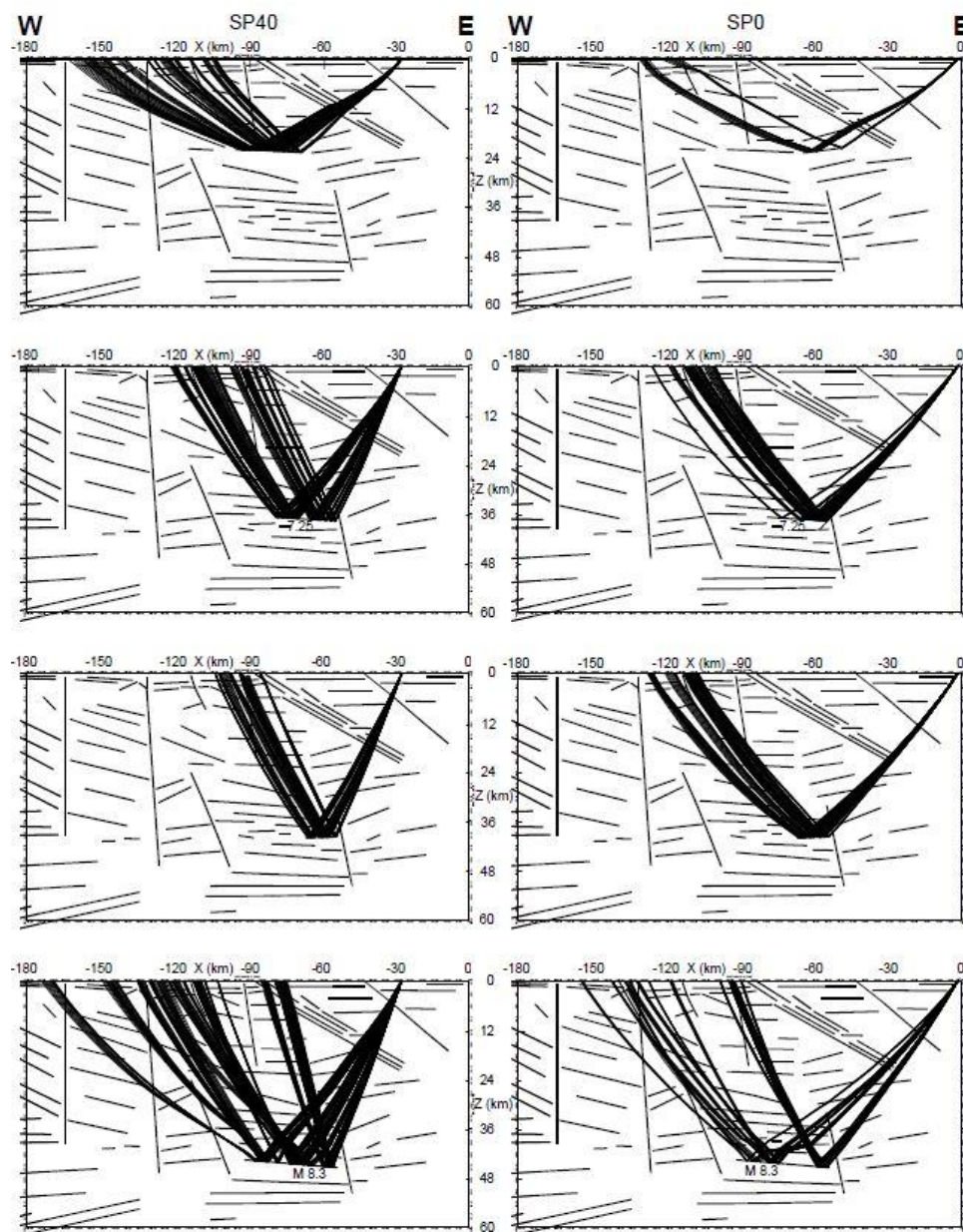


Figure 4c

Figure 4. (a, b). Ray-tracings from the reflector segments of the CEBT with its fine structure generated by our modeling approach from SP0, SP40 and SP80. Ray paths for reflections from each of the localized phantom horizon segments are generated for further computation of travel times and synthetic

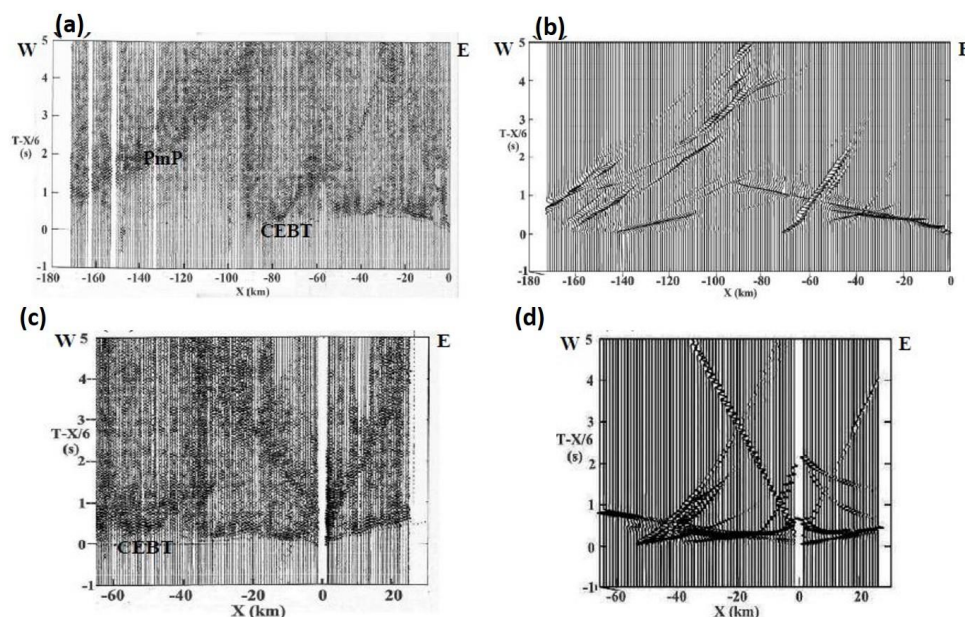


628 seismograms. The dips as well as locations of all the reflector segments in the section are kept unchanged,
629 varying only the velocity contrast across each one of them to generate the reflected waves, starting from
630 reflectors at the shallow to deeper depths. (c). Ray-tracings from SP0 and SP40 illustrated for a few of
631 the reflector segments in the middle and lower crust as well as the Moho (M) to demonstrate our new
632 approach.

633

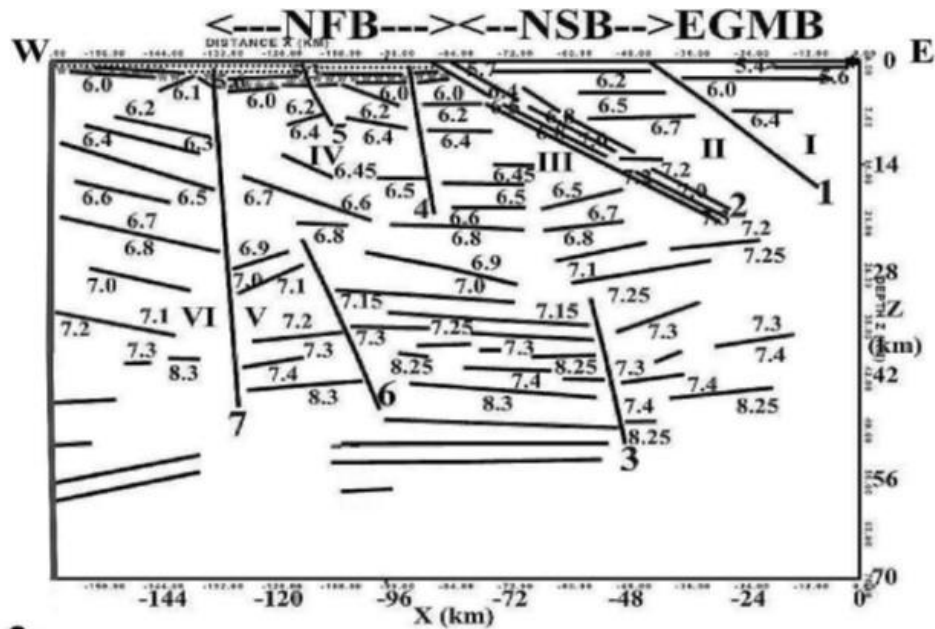


634



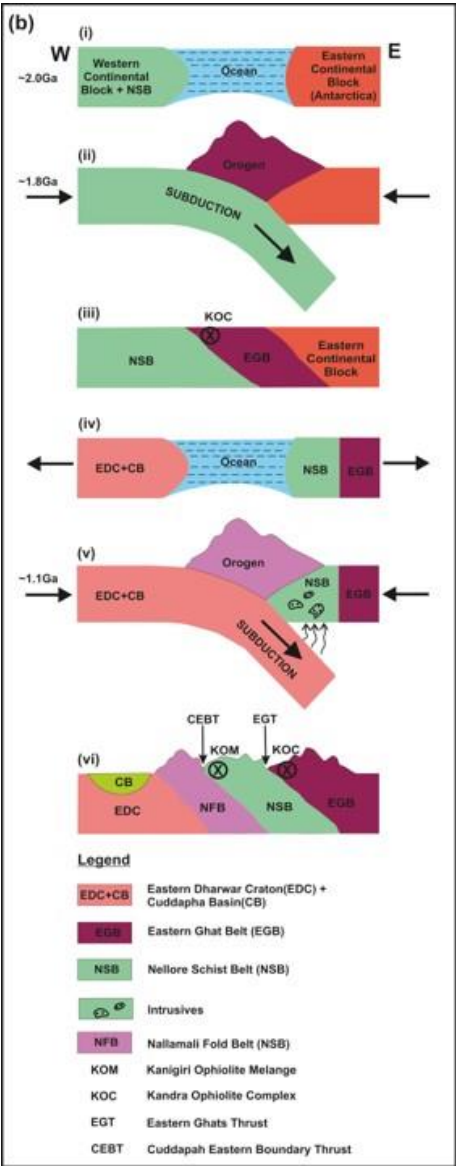
635

Figure 5. Observed and the Gaussian Beam synthetic seismogram sections especially revealing the CEBT, (a, b) from SP0 and (c, d) from SP40. The original field analog seismic traces were digitized (Krishna and Kaila, 1986) with a sampling rate of 250 samples per second and plotted as record sections using a reduction velocity of 6 km/s. The observed seismic record sections from (a) SP0 and (c) SP40, as well as their synthetics, (b) SP0 and (d) SP40, presented here for the first time, reveal unequivocal reflection signatures of the low-angle thrust fault CEBT. As can be seen from (a), the observed significant high-amplitude and high-apparent velocity CEBT reflection phase is as prominent as the Moho reflection phase PmP.



644

645 **Figure 6a.** P wave velocity structural model of the crust and geometry (including some inferred layering
646 within) of the thrust-fault CEBT obtained for the first time by the new modeling approach developed here.
647 This model confirms the high velocity (6.8 - 7.3 km/s) structure of the CEBT. The gross structural features
648 including the deep faults of the continental crust inferred earlier (Kaila et. al., 1979) are retained here,
649 with only the large number of smaller discrete reflector segments (Figure 3a) being replaced by fewer
650 localized phantom horizons (Figure 3b) in the new modeling approach. The deep crustal velocity
651 structure, not obtained earlier, is modelled here by the present approach. NFB: Nallamalai Fold Belt,
652 NSB: Nellore Schist Belt, EGMB: Eastern Ghats Mobile Belt, 6.4 P velocity km/s, 1, 2 Thrust Faults, 3-
653 7 Deep Faults, I-VI Crustal Blocks.



654

655 **Figure 6b.** A schematic model illustrating the geodynamic evolutionary scenario of the Cuddapah basin
656 derived by the seismic structures obtained here and other geological data as discussed in the text. (i) The
657 eastern continental block (Antarctica) was separated by an ocean from the western continental block
658 containing the Nellore Schist Belt (NSB). (ii) The western block was subducted to the east and collided
659 with the eastern block with the formation of Eastern Ghats Orogen at ~1.8 Ga. (iii) Combined continental
660 block showing the Eastern Ghats Thrust (EGT) and Kandra Ophiolite Complex (KOC) located between
661 the Nellore Schist Belt and Eastern Ghats Belt. (iv) opening of an ocean between the combined Eastern



662 Dharwar Craton (EDC) and Cuddapah Basin (CB) block and the eastern Continental block consisting of
663 NSB and EGB. (v) Subduction of EDC towards the east and subsequent collision between western and
664 Eastern blocks resulted in the formation of Nallamalai Fold Belt (NFB) at ~1.1 Ga. (vi) Present day
665 structure shows the low-angle thrust-fault, Cuddapah Eastern Boundary Thrust (CEBT), formed during
666 the 1.1 Ga collisional episode on the eastern margin of the Cuddapah basin. Locations of 1.8 Ga Kandra
667 ophiolite Complex (KOC) and 1.1 Ga Kanigiri ophiolite Melange (KOM) are also shown. Evidence for
668 the presence of ocean is derived from two periods of ophiolites and available literature referred in the
669 text.